Path Dependence of AMOC Weakening: A Geostrophic Shear Approach

Yuchen Li | Tesla STEM High School, Redmond, WA, USA

Introduction

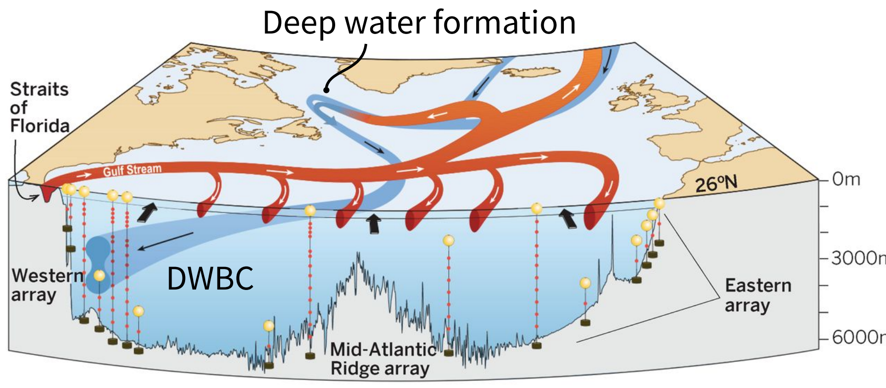

Above: AMOC cross section schematic. Adapted from Srokosz and Bryden, 2015.

NCAR | UCAR | COMMUNITY EARTH SYSTEM MODEL CESM ®

AMOC (Atlantic Meridional Overturning Circulation) is a crucial component of the climate system.

⇩

The mean AMOC strength is projected to weaken in the next century.

⇩

Understanding its response (e.g., mechanisms, variability, trend, etc.) to forcing is crucial.

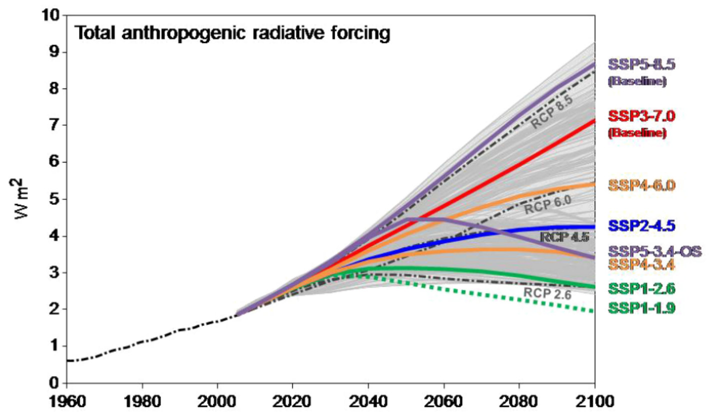

Above: radiative forcing in the Shared Socioeconomic Pathways (SSPs). (O'Niell)

Research question:

How, and to what degree, does AMOC weaken in different forcing pathways (SSP scenarios)?

Methodology

Strategy: AMOC is forced by complex factors. Instead, we can analyze it by calculating an approximate streamfunction (volume transport) from density and wind. This allows us to manipulate and diagnose AMOC trends and variability through the lens of forcing mechanisms (e.g., changing T and S fields).

Decomposition of AMOC: $\Psi_{\text{AMOC}} = \Psi_g + \Psi_{Ek} + \Psi_{ext}$

Geostrophic shear component, driven by zonal boundary densities

Ekman component, driven by wind

External mode component, driven by bottom velocities

The geostrophic shear component is the main component and can be calculated by integrating the geostrophic shear (thermal wind) relation.

$$f\frac{\partial v}{\partial z} = -\frac{g}{\rho^*}\frac{\partial \rho}{\partial x}$$

f : Coriolis parameter
ρ : density
g : gravitational acceleration
v : northward velocity

Two methods were attempted. Method B is altered after the formulation in Waldman et al., 2021.

Method A: rough approximation. Assume AMOC trend is driven by Ψ_g, which is dependent on boundary densities.

$$\Psi_{\text{AMOC}} \approx \Psi_{g, v(-h)=0}$$

Method B: better approximation. Calculate Ψ_g and Ψ_{Ek} compensated with barotropic flow by no-net-flow.

$$\Psi_{\text{AMOC}} \approx \Psi_g + \Psi_{Ek}$$

⇩

Method B has better trend and variability reproduction on almost all latitudes.

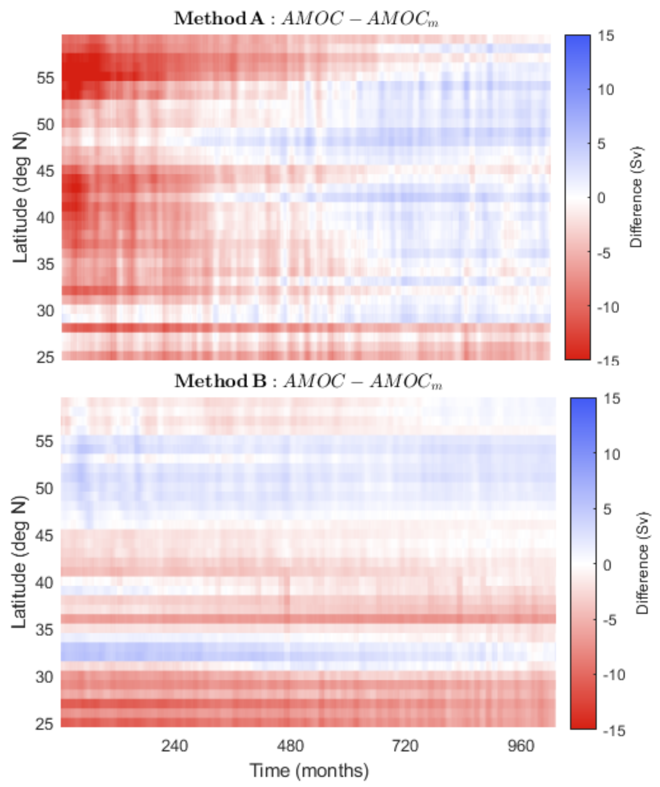

Above: reconstructed AMOC minus true AMOC plotted over time. Note trend discrepancies in Method A.

Latitudes where the reconstruction does not closely approximate the true AMOC were filted out using the following metrics:

$$\left|\text{mean}\left(\frac{\text{AMOC}_\text{m} - \text{AMOC}}{\text{AMOC}_\text{m}}\right)\right| < 0.25, \quad \left|\frac{\text{std(AMOC)}}{\text{std(AMOC}_\text{m})} - 1\right| < 0.20$$

$$p = 1 - \text{tCDF}(T, n-1) < 0.05$$

Results

The geostrophic shear component may be isolated in terms of temperature-driven and salinty-driven density change.

$$\Delta\rho(t) = \rho(t) - \rho_0 = \Delta\rho_S(t) + \Delta\rho_T(t)$$
$$\Delta\rho_T(t) = -\alpha\Delta\Theta(t)\rho_0$$
$$\Delta\rho_S(t) = \beta\Delta S_A(t)\rho_0$$

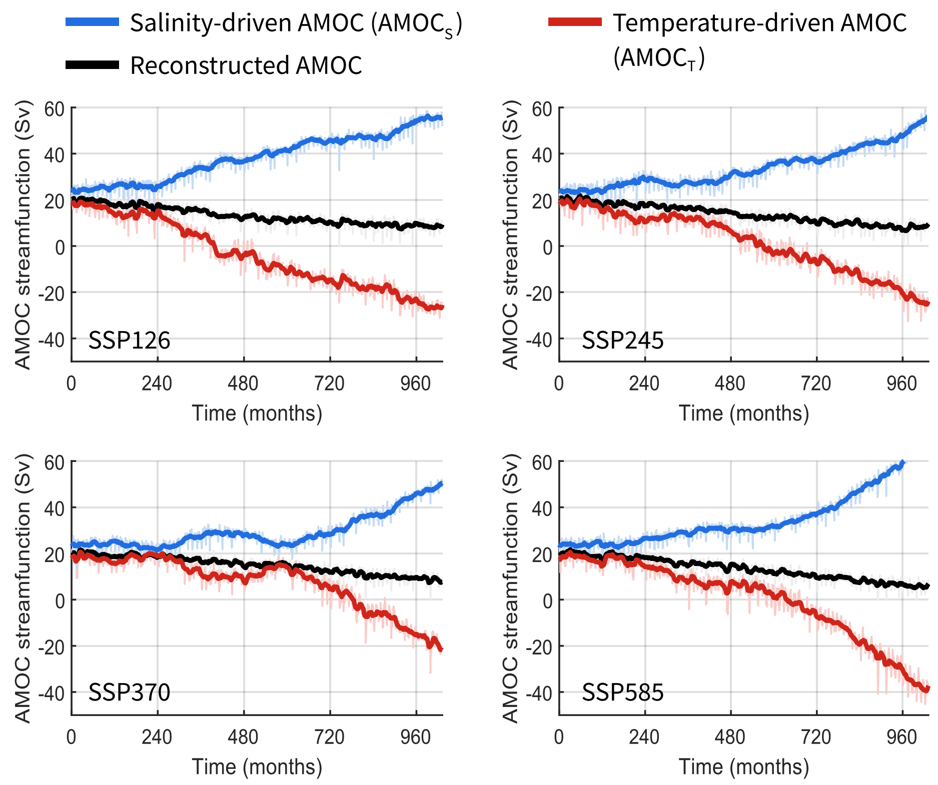

Fig 1: decomposition of salinity-driven and temperature-driven AMOC at 33.5 deg N as calculated from density using Method B. Overall AMOC is shown in black.

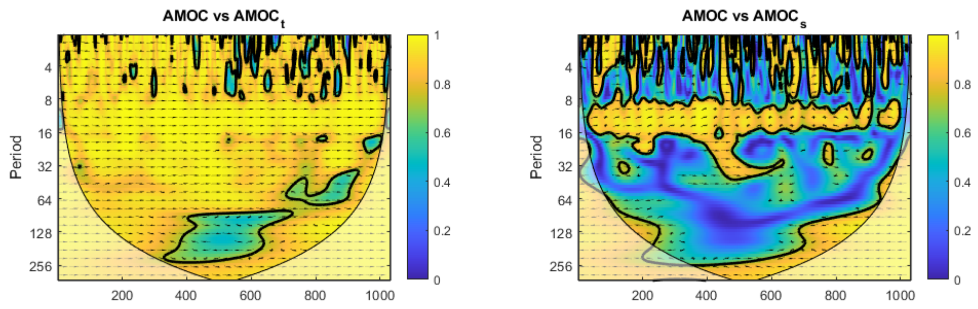

Fig 4: wavelet coherence between AMOC its temperature-driven (left) and salinity-driven (right) components. This suggests variability is mostly temperature driven.

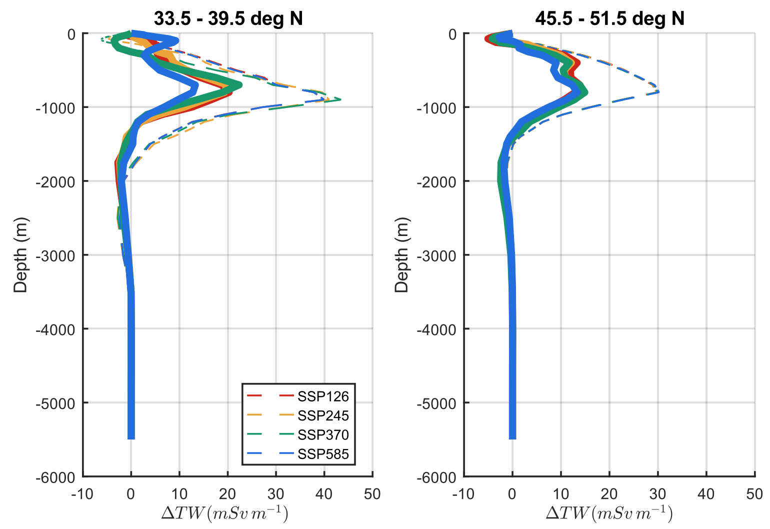

Fig 2: thermal wind (TW) profiles in two latitude bands. Dashed lines show start (2015) values and solid line show end (2100) values.

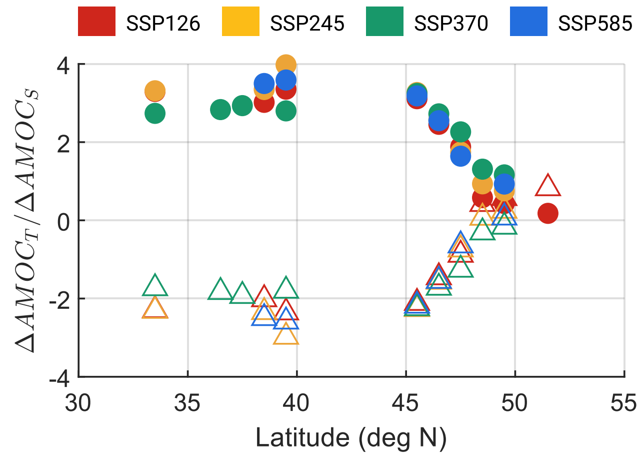

Fig 3: meridional profile of temperature- (dots) and salinity- (triangles) driven AMOC change. Note the opposing sign.

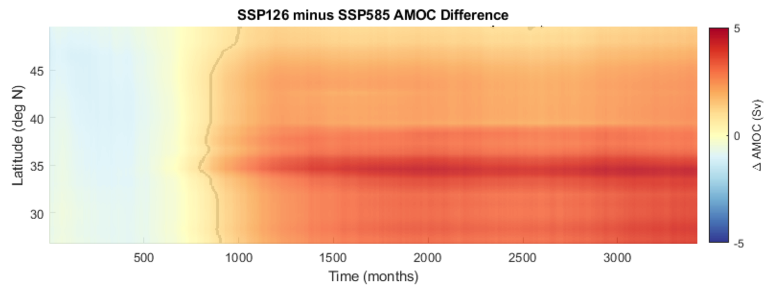

Fig 5: latitude-time plot of the AMOC streamfunction in SSP126 minus SSP585. The contour denotes a difference of 1 Sv.

Conclusions

- AMOC decline and AMOC variability in the CESM2 SSP simulations is **thermally** driven; salinity changes act to oppose this, but weakening dominates (Fig 1, 3)
- Density-driven AMOC decline is most pronounced near the depth of maximum overturning (Fig 2)
- TW profiles show weakening is likely driven by both upper limb (e.g., Gulf Stream) and lower limb (e.g., DWBC) dynamics
- The divergence of AMOC trends greatly lags divergence in forcing (Fig 6); this lag is meridionally constant (Fig 5)

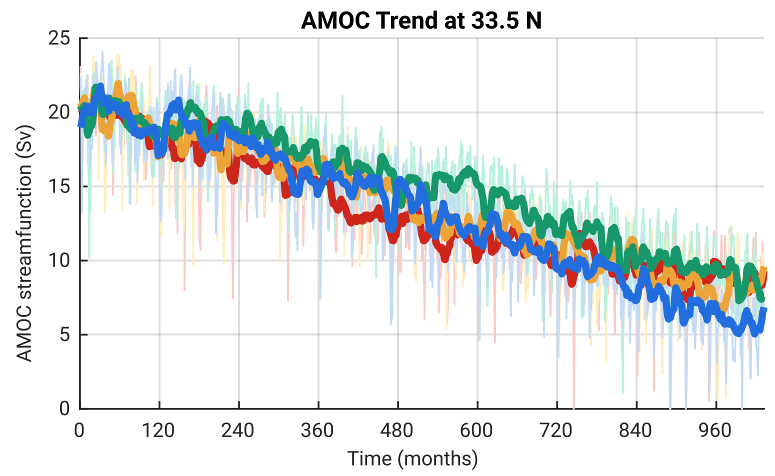

Fig 6: AMOC timeseries at 33.5 N. Note the similar trends regardless of forcing pathway.

Limitations & future opportunities

This was a single-model study ⇨ Expand framework to the complete CMIP6 model ensemble ⇨ Reduces effect of internal model variability, better assessment of AMOC trends among state-of-the-art models

In-depth analysis of scenario extension runs ⇨ Better understanding of mechanisms behind lag in AMOC trend divergence ⇨ Better predictability of future AMOC, to direct policy/aid towards mitigating negative impacts of AMOC decline